Dentomaxillofacial Radiology (2015) 44, 20150018

birpublications.org/dmfr

RESEARCH ARTICLE

Measuring absorbed dose for i-CAT CBCT examinations in child, adolescent and adult phantoms

E Choi and N L Ford

Department of Oral Biological and Medical Sciences, The University of British Columbia, Vancouver, BC, Canada

Objectives: Design and construct child and adolescent head phantoms to measure the absorbed doses imparted during dental CBCT and compare with the absorbed dose measured in an adult phantom.
Methods: A child phantom was developed to represent the smallest patients receiving CBCT, usually for craniofacial developmental concerns, and an adolescent phantom was developed to represent healthy orthodontic patients. Absorbed doses were measured using a thimble ionization chamber for the custom-built child and adolescent phantoms and compared with measurements using a commercially available adult phantom. Imaging was performed with an i-CAT Next Generation (Imaging Sciences International, Hatfield, PA) CBCT using two different fields of view covering the craniofacial complex (130 mm high) or maxilla/mandible (60 mm high).
Results: Measured absorbed doses varied depending on the location of the ionization chamber within the phantoms. For CBCT images obtained using the same protocol for all phantoms, the highest absorbed dose was measured in all locations of the small child phantom. The lowest absorbed dose was measured in the adult phantom.
Conclusions: Images were obtained with the same protocol for the adult, adolescent and child phantoms. A consistent trend was observed with the highest absorbed dose being measured in the smallest phantom (child), while the lowest absorbed dose was measured in the largest phantom (adult). This study demonstrates the importance of child-sizing the dose by using dedicated paediatric protocols optimized for the imaging task, which is critical as children are more sensitive to harmful effects of radiation and have a longer life-span post-irradiation for radiation-induced symptoms to develop than do adults.
Dentomaxillofacial Radiology (2015) **44**, 20150018. doi: 10.1259/dmfr.20150018

Cite this article as: Choi E, Ford NL. Measuring absorbed dose for i-CAT CBCT examinations in child, adolescent and adult phantoms. *Dentomaxillofac Radiol* 2015; **44**: 20150018.

Keywords: paediatric dentistry; radiology; radiation dosimetry; radiographic phantoms

Introduction

The most advertised merit of dental CBCT is that it emits a low or reduced radiation dose, which is true in comparison to multidetector CT (MDCT). Conventional MDCT requires multiple rotations for a single scan, whereas a CBCT scan only requires one rotation, thus decreasing the radiation. The conventional head MDCT effective dose is reported to be approximately 314–2426 μSv,[1,2] which is much higher than reported effective doses of 36.9–1073.0 μSv for CBCT of the mandible or maxilla.[2,3] These doses vary widely depending on the field of view (FOV), resolution, scan time, X-ray tube voltage (kVp) and current (mA) selected. Radiation doses from full FOV dental CBCT scans have been reported to range from 2% to 23% of doses of MDCT examinations.[4] Recently, Deman et al[5] measured the absorbed dose in MDCT and dental CBCT, holding the scan parameters and scan length constant. They found that the normalized absorbed dose for a 100-mAs exposure in MDCT was

Correspondence to: Dr Nancy Lee Ford. E-mail: nlford@dentistry.ubc.ca

Funding for this project was from the UBC Faculty of Dentistry Research Equipment Grant (2011) and the UBC Faculty of Dentistry Research Fund.
Received 15 January 2015; revised 9 March 2015; accepted 17 March 2015

double the normalized absorbed dose for CBCT,[5] but the difference may be more pronounced for clinical conditions, as the MDCT typically operate at higher mAs to ensure good soft-tissue contrast.

If dental CBCT use was limited to replacing medical CT for craniofacial visualization, the total radiation dose to the patient would indeed be reduced.[6] However, dental CBCT is often used to supplement conventional radiography such as bitewing, periapical, panoramic and cephalometric radiographs. The radiation doses from full FOV dental CBCT scans have been measured to be 4–42 times the dose from a panoramic radiograph.[4,5] Therefore, the clinicians ordering dental CBCT should be mindful that frequent use of supplemental CBCT results in non-negligible increases in the total radiation dose to the patient. Conclusions of a 2009 systematic review demonstrated that the most common uses of dental CBCT are for maxillofacial surgery (41%), dentoalveolar pathology (29%), orthodontics (16%) and implantology (13%).[7] In maxillofacial surgery, common uses of CBCT include temporomandibular joint assessment, arthrography, odontogenic cysts and tumours, trauma, cleft pathology, orthognathic surgery, oral cancer, osteomyelitis, bisphosphonate-related osteonecrosis of jaw and obstructive sleep apnoea.[7] For orthodontic purposes, mini-implant, cephalometry and tooth positions were the most common indications for CBCT scans.[7]

An increasing number of CBCT images are being performed on children and adolescents, which is concerning as children are more sensitive to radiation,[8,9] particularly the thyroid gland, gonads and breast tissue, and the cancer risk per Sievert is highest at a younger age and decreases with age.[10] In medical radiology, the Image Gently campaign has increased the awareness of radiation safety in paediatric populations[11] and has recently been extended to include dental radiology procedures. To address the important goals of the Image Gently campaign, paediatric protocols should be designed that will reduce the dose to the patient without compromising the diagnostic quality of the images.

The aim of our study was to investigate the X-ray dose received by a variety of adult and paediatric patients and to estimate the dose reduction that could be achieved with paediatric protocols. The authors developed dosimetry phantoms for measuring the absorbed dose imparted during dental CBCT examinations of child and adolescent patients. The authors compared the absorbed dose measured in our child and adolescent phantoms with a commercially available adult head phantom using a fixed imaging protocol.

Methods and materials

All phantoms were cylindrical in shape and made of polymethyl methacrylate (PMMA), which is a transparent thermoplastic material. PMMA shows similar energy absorption to muscle and water content of the maxillofacial region. All phantoms had holes drilled through the height of the cylinder to enable insertion of an ionization chamber. Custom-built phantoms (British Columbia Cancer Agency, Genome Sciences Centre, Vancouver, Canada) were made to represent the paediatric population. The adolescent phantom was designed to represent a 12-year-old child, consistent with entry into orthodontic treatment. The adolescent phantom was 135 mm in diameter and 150 mm in height, with 12.5-mm diameter holes for the ionization chamber. The child phantom represents a 5-year-old child, consistent with the youngest patients receiving CBCT in the dental clinics associated with the University of British Columbia Faculty of Dentistry. The child phantom was identical to the adolescent phantom except that the diameter was 100 mm. The adult-sized phantom was the SEDENTEX CT DI (Leeds Test Objects, Ltd, York, UK). The adult phantom measures 150 mm in diameter and 160 mm in height, with holes measuring 26 mm in diameter. The phantoms and experimental set-up are shown in Figure 1.

Imaging was performed using an i-CAT Next Generation (Imaging Sciences International, Hatfield, PA) CBCT machine. All images were obtained with the same parameters (120 kVp; 5 mA; exposure time, 4 s; voxel spacing, 0.4 mm) with two FOVs. On this unit, the FOV has a constant diameter of 160 mm, and the authors chose the large (130-mm height) and medium (60-mm height) settings, representing imaging the craniofacial complex or the mandible/maxilla, respectively.

Each phantom was placed on a PMMA plate that was mounted onto a tripod for positioning in the CBCT machine. The phantom was centred within the FOV using the positioning lasers. A thimble ion chamber (10×6-0.6-CT; Radcal Corporation, Monrovia, CA) was positioned in the selected hole, using an adaptor for the adult phantom to ensure that the chamber was completely surrounded by PMMA. The chamber was connected to an Accu-Dose meter (model 2186 v. 7.03; Radcal Corporation) for measuring the exposure. The ion chamber was factory calibrated to be within ±5% over the range of energies used in diagnostic CT. All measurements were obtained using the high-sensitivity setting for improved accuracy at the observed dose rate.

Exposure measurements were obtained at the centre of the phantom and at the periphery and converted to absorbed dose in PMMA. The ion chamber was also taped to the outer surface of the phantom, and exposure was converted to absorbed dose in air. Measurements at the periphery and on the phantom surface were obtained on the anterior, posterior, left and right sides of the phantom head. Measurements from three images were averaged together to yield a point dose at each location. Descriptive statistics are reported, including the mean, minimum and maximum values of the absorbed doses, along with the standard deviations of the measurements.

Results

The exposure was measured and converted into absorbed dose to the PMMA phantom for the measurements

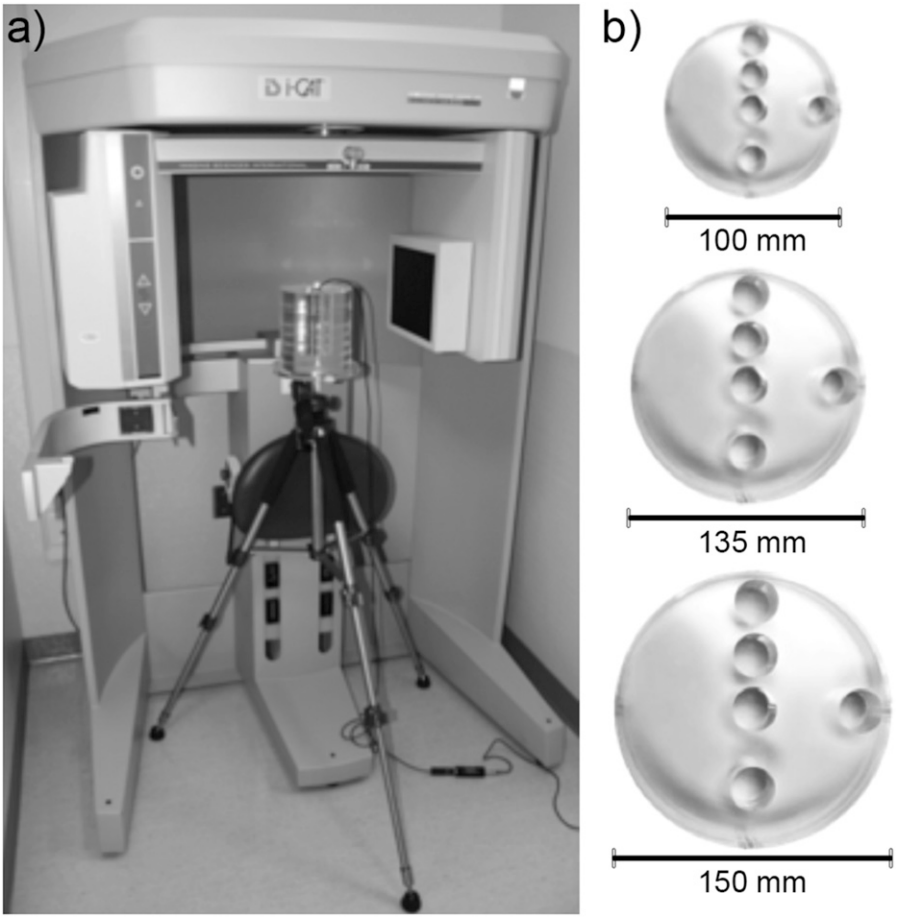

Figure 1 (a) Adult head phantom mounted on the tripod and positioned in the CBCT scanner. The cord connects the ion chamber to the dosemeter. (b) Top views of the child (top—100-mm diameter), adolescent (middle—135-mm diameter) and adult (bottom—150-mm diameter) phantoms. Each phantom can be rotated on the tripod to position the ion chamber hole at the desired location for dosimetry.

inside the phantom. For the measurements obtained on the surface of the phantom, the exposure values were measured and converted into the absorbed dose in air. The average, maximum and minimum absorbed doses are tabulated in Table 1 for the 160-mm diameter by 60-mm high FOV and in Table 2 for the 160-mm diameter by 130-mm high FOV. As expected, the absorbed doses measured in the craniofacial FOV (160-mm diameter by 130-mm high) were larger than in the mandible/maxilla FOV (160-mm diameter by 60-mm high).

The values reported in the centre of the phantom represent an average of three measurements. For the periphery and surface values, measurements were repeated three times at four different locations, representing the front, back, left and right sides of a patient. Since the phantom is cylindrical in shape and the imaging settings used a full rotation to obtain projections, the measurements were similar in all 4 locations, and all 12 measurements were combined to yield a single value representing all locations at the same radial distance. For different imaging systems, the measured values across the patient's head may not be similar, depending on the orbit of the X-ray tube. All of the measured values from the same location were very similar as shown by the small values for the standard deviations, indicating good reproducibility of the X-ray exposure between images.

In every measurement location, the highest absorbed doses were measured in the child phantom, with the lowest values measured in the adult phantom. In the results reported here, it is clear that the smallest head diameter received the largest radiation dose under identical imaging conditions. These results can be explained by a couple of reasons. First, the larger diameter of the adult phantom absorbed more radiation at the edges of the FOV, whereas the adolescent and child phantoms had less PMMA to absorb the radiation, allowing more radiation to penetrate to the centre. In both Tables 1 and 2, the average dose values at the centre are higher in the smaller phantoms (child and adolescent) than in the adult phantom. Secondly, the X-ray beam carries more energy along the central axis than at the edges of the FOV. This implies that less radiation will reach the portions of the phantoms at the edges of the FOV, which would more strongly impact the adult phantom owing to its larger diameter. The surface values for the adult phantom are lower than the

Table 1 i-CAT Next Generation (Imaging Sciences International, Hatfield, PA) CBCT radiation measurement: field of view, 60-mm high × 160-mm diameter; 120 kVp; 5 mA; 0.4 voxel; and 4 s exposure time

Phantom	*Location*	*Absorbed dose average (mGy)*	*Absorbed dose maximum (mGy)*	*Absorbed dose minimum (mGy)*
Adult	Centre	1.10 ± 0.002	1.11	1.10
	Periphery	1.31 ± 0.02	1.33	1.29
	Surface	1.33 ± 0.07	1.43	1.25
Adolescent	Centre	1.53 ± 0.002	1.53	1.53
	Periphery	1.65 ± 0.05	1.70	1.59
	Surface	1.58 ± 0.04	1.63	1.54
Child	Centre	1.85 ± 0.01	1.86	1.84
	Periphery	1.88 ± 0.04	1.93	1.83
	Surface	1.97 ± 0.03	2.00	1.93

The centre and periphery measurements are absorbed dose in polymethyl methacrylate and the surface measurements are absorbed dose in air. Mean ± standard deviation, maximum and minimum measured values are reported at each location.

corresponding measurements using both the adolescent and child phantoms.

Table 3 shows the average dose values as a percentage of the adult dose. In each case, the dose values for the child and adolescent phantoms are higher than the corresponding locations in the adult phantom, leading to percentages >100%. In this table, it is clear that reducing the dose to the child and adolescent phantoms to the level received by adults would result in dose savings of 18–47% in adolescents and 37–68% for smaller children. The dose could be further reduced in smaller patients, as less radiation is needed to penetrate the volume of tissue and produce diagnostic images. By creating child and adolescent imaging protocols, dose savings of up to 50–70% could be realized. To create these protocols, image quality must also be assessed alongside the dose measurements to ensure that the important details needed for diagnostic purposes are not lost.

Discussion

In this study, the authors compare the absorbed dose measured at different locations inside PMMA head phantoms that represent adult, adolescent and child patients. All imaging was performed on the same CBCT unit, with identical X-ray tube and image resolution settings and using two different FOVs, demonstrating the absorbed dose measured for craniofacial or maxilla/mandible imaging. The adult phantom attenuated more radiation owing to its size (diameter)[12] than did the adolescent or paediatric phantoms, as expected. Our measurements showed that more radiation reached the centre of the phantom as the diameter decreased. When the same imaging protocols were used for all three phantoms, the highest absorbed doses were measured in the small child phantom in all measurement locations. Knowing children's sensitivity to radiation and risk involved, one should weigh the risk and benefit carefully before ordering CBCT imaging for children. Only when two-dimensional imaging is inconclusive or impractical should a CBCT image be considered.

In a previous study that compared adult and child radiation equivalent doses from two different dental CBCT units, different amounts of radiation were measured depending on the CBCT devices, location of centre, size and FOV.[8] When the same CBCT imaging protocol was used for both children and adults, higher radiation was measured in the head and neck of children than in those of adults.[13,14] Our study showed the same trend for the absorbed dose, although measured in a uniform PMMA phantom in a single imaging plane; nonetheless, our study demonstrates the importance of using a paediatric imaging protocol for children and adolescents.

It is difficult to compare the measurements from this study to measurements from other studies owing to the variety of dose metrics employed. Many articles investigating dental CBCT dosimetry use effective dose

Table 2 i-CAT Next Generation (Imaging Sciences International, Hatfield, PA) CBCT radiation measurement: field of view, 130-mm high × 160-mm diameter; 120 kVp; 5 mA; 0.4 voxel; and 4 s exposure time

Phantom	*Location*	*Absorbed dose average (mGy)*	*Absorbed dose maximum (mGy)*	*Absorbed dose minimum (mGy)*
Adult	Centre	1.33 ± 0.002	1.33	1.33
	Periphery	1.52 ± 0.02	1.54	1.49
	Surface	1.48 ± 0.07	1.58	1.39
Adolescent	Centre	1.95 ± 0.01	1.95	1.94
	Periphery	1.93 ± 0.04	1.99	1.87
	Surface	1.74 ± 0.03	1.76	1.69
Child	Centre	2.20 ± 0.003	2.20	2.19
	Periphery	2.08 ± 0.04	2.14	2.00
	Surface	2.19 ± 0.03	2.23	2.16

The centre and periphery measurements are absorbed dose in polymethyl methacrylate and the surface measurements are absorbed dose in air. Mean ± standard deviation, maximum and minimum measured values are reported at each location

Table 3 Average absorbed dose values expressed as a percentage of the corresponding adult measurement

Phantom	*Field of view height (mm)*	*Centre (% of adult)*	*Periphery (% of adult)*	*Surface (% of adult)*
Child (100-mm diameter)	60	168	144	148
Child (100-mm diameter)	130	165	137	148
Adolescent (135-mm diameter)	60	139	126	119
Adolescent (135-mm diameter)	130	147	127	118

Values >100% indicate higher doses than those measured in the corresponding location of the adult phantom.

despite the fact that the absorbed dose is a better metric. Effective dose is a measure of radiation risk that is inadequate for use in paediatric patients because it does not take demographic factors such as gender, age and body composition into consideration. In addition, previous studies show that effective doses are clinically very complex to obtain and have low reproducibility,[15] which can be attributed to difficulty in aligning the locations of organs of interest and thermoluminescent devices.[16] Other metrics reported are the dose–area product and the CT dose index. The dose–area product is a measurement of tube output, and therefore not related to the patient dose but is commonly displayed at the acquisition console during the image acquisition. The CT dose index is related to the dose metric used in MDCT; however, this metric is not valid in the cone beam geometry. Recently, Dixon et al[17] proposed a new method for measuring the absorbed dose in CBCT systems, which has been applied to dental CBCT by Deman et al.[5]

In this study, the authors reported the absorbed dose, because it is a measurement of the energy imparted to the phantoms and is readily compared with the dose metrics used with CBCT machines located in radiology departments. The absorbed dose can be used to calculate other metrics (dose–area product or effective dose), so the trends seen in this study will persist across other measurement techniques. The authors report the absorbed dose measured at a number of locations within the phantom in a single imaging plane. This information could be used to calculate the average dose similar to Deman et al;[5] however, examining the dose distribution within the phantom is also useful and demonstrates that the dose for child and adolescent patients is higher in every location than in the corresponding positions within the adult phantom. The doses reported here are likely underestimates compared with those received by patients owing to the uniform PMMA material used for the phantoms. The PMMA mimics soft tissue but does not absorb as much radiation as hard tissue, like teeth or bone. Therefore, the absorbed dose would be higher in hard tissue regions than the absorbed dose values given here. Although the PMMA cylindrical phantoms described here are similar to those commonly used in radiology departments to calculate absorbed dose, they are not anatomically representative of patient anatomy. To obtain more closely related measurements for a patient would require anthropomorphic phantoms similar to the RANDO® phantom (The Phantom Laboratory, Salem, NY); however, the RANDO phantom does not have the same patient sizes available and only accepts thermoluminescent dosemeter or film, which are both very dependent upon calibration and require separate readout equipment. Using an ionization chamber in a PMMA cylinder is easy to implement and generally more reproducible for routine dosimetry measurements than other device and phantom combinations.

Conclusion

While the absorbed doses measured in our study are specific to the i-CAT Next Generation CBCT and specific imaging protocols used, the overall trend of measuring higher absorbed doses in smaller head sizes will be seen with other CBCT machines and imaging protocols. When the imaging protocols were held constant, the highest absorbed dose was measured in all locations in the small child phantom and the lowest absorbed dose was measured in the adult phantom. This study illustrates the necessity of optimizing the imaging protocols to ensure that child and adolescent patients are not receiving a higher radiation dose than that required for diagnosis.

Acknowledgments

The authors acknowledge Dr Pierre Deman (UBC Faculty of Dentistry) for assistance with the dosimetry calculations and Dr Robin Coope (BCCA Genome Sciences Centre) for helping to develop the phantoms.

References

1. Dula K, Mini R, van der Stelt PF, Lambrecht JT, Schneeberger P, Buser D. Hypothetical mortality risk associated with spiral computed tomography of the maxilla and mandible. *Eur J Oral Sci* 1996; **104**: 503–10. doi: 10.1111/j.1600-0722.1996.tb00133.x
2. Ludlow JB, Davies-Ludlow LE, Brooks SL. Dosimetry of two extraoral direct digital imaging devices: NewTom cone beam CT and Orthophos Plus DS panoramic unit. *Dentomaxillofac Radiol* 2003; **32**: 229–34. doi: 10.1259/dmfr/26310390
3. Ludlow JB, Ivanovic M. Comparative dosimetry of dental CBCT devices and 64-slice CT for oral and maxillofacial radiology. *Oral Surg Oral Med Oral Pathol Oral Radiol Endod* 2008; **106**: 106–14. doi: 10.1016/j.tripleo.2008.03.018
4. Ludlow JB, Davies-Ludlow LE, Brooks SL, Howerton WB. Dosimetry of 3 CBCT devices for oral and maxillofacial radiology: CB Mercuray, NewTom 3G and i-CAT. *Dentomaxillofac Radiol* 2006; **35**: 219–26. doi: 10.1259/dmfr/14340323

5. Deman P, Atwal P, Duzenli C, Thakur Y, Ford NL. Dose measurements for dental cone-beam CT: a comparison with MSCT and panoramic imaging. *Phys Med Biol* 2014; **59**: 3201–22. doi: 10.1088/0031-9155/59/12/3201
6. Chau AC, Fung K. Comparison of radiation dose for implant imaging using conventional spiral tomography, computed tomography, and cone-beam computed tomography. *Oral Surg Oral Med Oral Pathol Oral Radiol Endod* 2009; **107**: 559–65. doi: 10.1016/j.tripleo.2008.11.009
7. De Vos W, Casselman J, Swennen GR. Cone-beam computerized tomography (CBCT) imaging of the oral and maxillofacial region: a systematic review of the literature. *Int J Oral Maxillofac Surg* 2009; **38**: 609–25. doi: 10.1016/j.ijom.2009.02.028
8. Al Najjar A, Colosi D, Dauer LT, Prins R, Patchell G, Branets I, et al. Comparison of adult and child radiation equivalent doses from 2 dental cone-beam computed tomography units. *Am J Orthod Dentofacial Orthop* 2013; **143**: 784–92. doi: 10.1016/j.ajodo.2013.01.013
9. Pierce DA, Preston DL. Radiation-related cancer risks at low doses among atomic bomb survivors. *Radiat Res* 2000; **154**: 178–86. doi: 10.1667/0033-7587(2000)154[0178:rrcral]2.0.co;2
10. Hall EJ, Giaccia AJ. *Radiobiology for the radiologist*. Philadelphia, PA: Lippincott Williams & Wilkins; 2006.
11. Goske MJ, Applegate KE, Boylan J, Butler PF, Callahan MJ, Coley BD, et al. The "Image Gently" campaign: increasing CT radiation dose awareness through a national education and awareness program. *Pediatr Radiol* 2008; **38**: 265–9. doi: 10.1007/s00247-007-0743-3
12. Strauss K. Radiation safety summit—method to estimate radiation dose to pediatric patients from CT scans. *Pediatr Radiol* 2011; **41**: 210–11. doi: 10.1007/s00247-011-1978-6
13. Committee to Assess Health Risks from Exposure to Low Levels of Ionizing Radiation, National Research Council. *Health risks from exposure to low levels of ionizing radiation: BEIR VII phase 2*. Washington, DC: The National Academies Press; 2006.
14. Prins R, Dauer LT, Colosi DC, Quinn B, Kleiman NJ, Bohle GC, et al. Significant reduction in dental cone beam computed tomography (CBCT) eye dose through the use of leaded glasses. *Oral Surg Oral Med Oral Pathol Oral Radiol Endod* 2011; **112**: 502–7. doi: 10.1016/j.tripleo.2011.04.041
15. Lofthag-Hansen S, Thilander-Klang A, Ekestubbe A, Helmrot E, Gröndahl K. Calculating effective dose on a cone beam computed tomography device: 3D Accuitomo and 3D Accuitomo FPD. *Dentomaxillofac Radiol* 2008; **37**: 72–9. doi: 10.1259/dmfr/60375385
16. Cheng HC, Wu VW, Liu ES, Kwong DL. Evaluation of radiation dose and image quality for the Varian cone beam computed tomography system. *Int J Radiat Oncol Biol Phys* 2011; **80**: 291–300. doi: 10.1016/j.ijrobp.2010.06.014
17. Dixon RL, Anderson JA, Bakalyar DM, Boedeker K, Boone JM, Cody DD, et al. *Comprehensive methodology for the evaluation of radiation dose in x-ray computed tomography*. College Park, MD: American Association of Physicists in Medicine; 2010.